Table S1. Primer sequences used for cloning.

Primer	Sequence 5′-3′
pET22b GSSS RPCR Fwd	TCATCGCACCACCACCACCACCAC
pET22b GSSS RPCR Rev	AGAGCCCATATGTATATCTCCTTCTTAAAGTTA AACAAAATTATTTCTAG
ZIKV CO NS5 Fwd	GGAGATATACATATGGGGGGTGGCACTGGTG
ZIKV CO NS5 Rev	GTGCGATGAAGAGCCCAGTACGCCAGGTGTGG AAC
pET22b CO RPCR Fwd	GGCTCTTCATCGCACCAC
pET22b CO RPCR Rev	CATATGTATATCTCCTTCTTAAAGTTAAACAAA ATTATTTCTAGAGG
EcoRI-T7	GAATTCTAATACGACTCACTATAG
BamHI-HDVr	GGATCCCTTCTCCCTTAGCCTACCGAAG
ZIKV 5′ (+) Fwd	TACGACTCACTATAGAGTTGTTGATCTGTGTGA ATCAG
ZIKV 5′ (+) Rev	ATGCCATGCCGACCCCAGCATGGCAGCCAG
T7-HDVr RPCR Fwd	GGGTCGGCATGGCATCTC
T7-HDVr RPCR Rev	CTATAGTGAGTCGTATTAGAATTcgtaatcatgg
DENV1 3(-) Fwd	TACGACTCACTATAGCACGCGGTTTCTCGCGCG TTTC
DENV1 3(-) Rev	ATGCCATGCCGACCCAGTTGTTAGTCTACGTGG ACCGAC
DENV3 3(-) Fwd	TACGACTCACTATAGCACACGGTTTCTCACGCG TTTC
DENV4 3(-) Fwd	TACGACTCACTATAGCGGTTTCTCTCGCGTTTCA GC
DENV4 3(-) Rev	ATGCCATGCCGACCCAGTTGTTAGTCTGTGTGG ACCGAC
SLA GU Base RPCR Fwd	TCGGCAGGTTTTATTTTGGATTTGG
SLA GU Base RPCR Rev	TACCGTTGCTAGCTTTCGCTTC
SLA GU TSL Base RPCR Fwd	AGTTCGAGGGGGAAGCGAAAGCTAGCAAC
SLA GU TSL Base RPCR Rev	GTCGCAGAAGAATTCACACAGATCAACAAC
SLA GU TSL Top RPCR Fwd	GCGGGTCTGAAGCGAAAGCTAGCAAC
SLA GU TSL Top RPCR Rev	ACTGACATAGTCTGATTCACACAGATCAAC

Table S2. Geneblock sequences.

Geneblock	Sequence 5′-3′
ZIKV CO NS5 gBlock	GGGGGTGGCACTGGTGAGACCCTGGGGGAGAAGTGGAAAGCG CGCCTGAACCAGATGTCGGCCTTGGAGTTCTACTCCTACAAAA AAAGCGGCATCACGGAGGTTTGCCGGGAAGAAGCGCGGCGTG CGTTGAAGGATGGCGTCGCAACCGGGGGTCATGCGGTGTCTCG TGGTAGCGCAAAGCTCCGGTGGTTAGTGGAGCGTGGGTATCTG CAACCATACGGTAAAGTTATCGACTTAGGGTGCGGGCGCGGCG GTTGGTCGTACTACGTAGCCACAATCCGCAAGGTCCAGGAGGT AAAGGGTTACACGAAAGGCGGGCCAGGTCACGAAGAGCCTGT CCTTGTACAATCTTACGGCTGGAATATTGTGCGCCTCAAGTCCG GTGTCGACGTGTTCCACATGGCGGCGGAACCGTGCGATACCCT CTTATGCGATATCGGTGAGAGTAGCAGCTCCCCTGAAGTGGAG GAGGCCCGTACGTTGCGGGTATTATCGATGGTGGGTGACTGGT TAGAGAAACGTCCAGGGGCCTTCTGCATCAAAGTCCTGTGTCC ATATACATCTACAATGATGGAAACTCTTGAACGTCTCCAGCGC CGGTACGGGGGCGGGCTCGTCCGTGTTCCATTAAGCCGCAATT CTACACACGAGATGTATTGGGTGAGTGGGGCGAAATCGAACAC GATTAAAAGCGTTTCTACGACGTCTCAGTTGCTTCTTGGCCGTA TGGATGGTCCACGGCGCCCGGTCAAGTATGAAGAAGACGTTAA TCTGGGGAGTGGTACACGGGCCGTTGTCAGTTGTGCGGAAGCG CCGAACATGAAGATCATTGGCAACCGGATTGAGCGTATCCGCT CAGAACATGCAGAAACGTGGTTCTTTGATGAAAACCACCCTTA CCGGACCTGGGCTTACCACGGTAGCTACGAAGCTCCTACTCAA GGGTCTGCCTCGAGCTTAATTAATGGCGTGGTCCGGCTCCTGTC TAAGCCTTGGGATGTCGTAACGGGCGTCACCGGTATTGCCATG ACTGATACTACTCCATACGGGCAACAGCGTGTTTTTAAGGAGA AGGTGGACACCCGTGTTCCTGATCCGCAGGAGGGCACTCGTCA AGTGATGTCGATGGTTTCTAGCTGGCTGTGGAAGGAGCTGGGT AAACATAAACGCCCACGCGTCTGCACTAAGGAGGAGTTCATCA ATAAGGTTCGGTCGAACGCCGCGCTGGGCGCCATTTTCGAAGA GGAGAAGGAGTGGAAGACCGCGGTCGAAGCCGTGAATGACCC TCGTTTTTGGGCTCTGGTAGATAAGGAGCGTGAACATCATCTGC GCGGGGAATGTCAAAGTTGTGTATATAACATGATGGGCAAACG TGAAAAAAAGCAGGGCGAGTTCGGTAAAGCAAAAGGTAGTCG CGCGATCTGGTATATGTGGTTGGGCGCACGGTTTCTGGAATTTG AGGCTTTAGGGTTTTTGAATGAAGACCACTGGATGGGCCGCGA GAACAGTGGGGGCGGGGTGGAAGGGTTAGGGTTGCAACGCTT AGGGTACGTGCTGGAGGAGATGAGCCGTATTCCGGGGGGTCGC ATGTATGCCGACGATACTGCAGGTTGGGACACTCGGATCAGCC GGTTCGACTTGGAAAATGAGGCTCTCATTACCAATCAGATGGA GAAGGGCCATCGTGCGTTGGCGTTAGCAATCATCAAGTACACG TATCAAAATAAAGTTGTGAAGGTGCTTCGTCCAGCCGAGAAGG GGAAGACAGTTATGGACATCATCAGTCGCCAAGACCAACGCGG CTCTGGGCAGGTGGTCACTTACGCTCTGAACACTTTCACTAATC

	TCGTAGTACAACTCATCCGCAACATGGAAGCTGAGGAAGTGCT TGAGATGCAGGACCTTTGGCTTTTGCGCCGGTCAGAAAAGGTA ACTAATTGGCTGCAGTCTAATGGGTGGGATCGGCTGAAGCGTA TGGCGGTATCGGGGGATGATTGCGTTGTTAAGCCGATCGACGA CCGGTTCGCCCACGCTTTACGGTTTTTAAACGACATGGGGAAG GTTCGGAAGGATACGCAGGAGTGGAAGCCGAGTACGGGTTGG GATAATTGGGAGGAGGTGCCGTTTTGCAGTCACCATTTTAACA AGTTGCATTTAAAGGACGGGCGTTCAATCGTCGTCCCTTGTCGC CATCAGGATGAATTGATTGGCCGTGCTCGGGTAAGTCCGGGGG CCGGTTGGTCCATTCGTGAAACAGCTTGTCTTGCTAAGTCGTAC GCGCAGATGTGGCAGCTTCTGTACTTCCATCGTCGTGACTTACG TCTCATGGCTAACGCAATTTGCTCCTCCGTTCCTGTTGATTGGG TGCCAACGGGGCGGACTACATGGTCAATCCACGGCAAGGGCG AGTGGATGACTACGGAAGATATGCTGGTGGTCTGGAACCGCGT CTGGATTGAGGAGAATGACCACATGGAGGACAAGACACCGGT TACAAAGTGGACCGATATCCCGTATTTGGGGAAACGCGAAGAT CTGTGGTGTGGGTCTCTGATCGGTCATCGTCCTCGTACCACCTG GGCTGAAAATATTAAGAATACGGTTAATATGGTTCGCCGCATT ATCGGTGACGAGGAAAAATATATGGACTATCTTTCTACTCAGG TGCGTTACCTTGGCGAGGAGGGTTCCACACCTGGCGTACTG
DENV1 5pos gBlock	AAAAAGAATTCTAATACGACTCACTATAGAGTTGTTAGTCTAC GTGGACCGACAAGAACAGTTTCGAATCGGAAGCTTGCTTAACG TAGTTCTAACAGTTTTTTATTAGAGAGCAGATCTCTGATGAACA ACCAACGGAAAAAGACGGGTCGACCGTCTTTCAATATGCTGAA ACGCGCGAGAAACCGCGTGTCAACTGTTTCACAGTTGGCGAAG AGATTCTCAAAAGGATTGCTTTCAGGCCAAGGACCCATGAAAT TGGTGATGGCTTTTATAGCATTCCTAAGATTTCTAGCCATACCT CCAACAGCAGGAATTTTGGCTAGATGGGGCTCATTCAAGAAGA ATGGAGCGATCAAAGTGTTACGGGGTTTCAAGAAAGAAATCTA AGAAAGATCTGGCTGCCATGCTGGGGTCGGCATGGCATCTCCA CCTCCTCGCGGTCCGACCTGGGCTACTTCGGTAGGCTAAGGGA GAAGGGATCCAAA
DENV2 5pos gBlock	AAAAAGAATTCTAATACGACTCACTATAGAGTTGTTAGTCTAC GTGGACCGACAAAGACAGATTCTTTGAGGGAGCTAAGCTCAAC GTAGTTCTAACAGTTTTTTAATTAGAGAGCAGATCTCTGATGAA TAACCAACGGAAAAAGGCGAAAAACACGCCTTTCAATATGCTG AAACGCGAGAGAAACCGCGTGTCGACTGTGCAACAGCTGACA AAGAGATTCTCACTTGGAATGCTGCAGGGACGAGGACCATTAA AACTGTTCATGGCCCTGGTGGCGTTCCTTCGTTTCCTAACAATC CCACCAACAGCAGGGATATTGAAGAGATGGGGAACAATTAAA AAATCAAAAGCTATTAATGTTTTGAGAGGGTTCAGGAAAGAGA TAAGAAAGATCTGGCTGCCATGCTGGGGTCGGCATGGCATCTC CACCTCCTCGCGGTCCGACCTGGGCTACTTCGGTAGGCTAAGG GAGAAGGGATCCAAA
DENV3 5pos gBlock	AAAAAGAATTCTAATACGACTCACTATAGAGTTGTTAGTCTAC GTGGACCGACAAGAACAGTTTCGACTCGGAAGCTTGCTTAACG

	TAGTGCTGACAGTTTTTTATTAGAGAGCAGATCTCTGATGAACA ACCAACGGAAGAAGACGGGAAAACCGTCTATCAATATGCTGA AACGCGTGAGAAACCGTGTGTCAACTGGATCACAGTTGGCGAA GAGATTCTCAAAAGGACTGCTGAACGGCCAGGGACCAATGAA ATTGGTTATGGCGTTCATAGCTTTCCTCAGATTTCTAGCCATTC CACCAACAGCAGGAGTCTTGGCTAGATGGGGAACCTTCAAGAA GTCGGGGGCCATTAAGGTCCTGAAAGGCTTCAAGAAGGAGATC TAAGAAAGATCTGGCTGCCATGCTGGGGTCGGCATGGCATCTC CACCTCCTCGCGGTCCGACCTGGGCTACTTCGGTAGGCTAAGG GAGAAGGGATCCAAA
DENV4 5pos gBlock	AAAAAGAATTCTAATACGACTCACTATAGAGTTGTTAGTCTGT GTGGACCGACAAGGACAGTTCCAAATCGGAAGCTTGCTTAACA CAGTTCTAACAGTTTGTTTGAATAGAGAGCAGATCTCTGGAAA AATGAACCAACGAAAAAAGGTGGTTAGACCACCTTTCAATATG CTGAAACGCGAGAGAAACCGCGTATCAACCCCTCAAGGGTTGG TGAAGAGATTCTCAACCGGACTTTTTTCTGGGAAAGGACCCTT ACGGATGGTGCTAGCATTCATCACGTTTTTGCGAGTCCTTTCCA TCCCACCAACAGCAGGGATTCTGAAGAGATGGGGACAGTTGAA GAAAAATAAGGCCATCAAGATACTGATTGGATTCAGGAAGGA GAAGAAAGATCTGGCTGCCATGCTGGGGTCGGCATGGCATCTC CACCTCCTCGCGGTCCGACCTGGGCTACTTCGGTAGGCTAAGG GAGAAGGGATCCAAA
ZIKV 3neg gBlock	AAAAAGAATTCTAATACGACTCACTATAGCGTTTTAGCATATT GACAATCCGGAATCCTCCGGATTTCTTTTTTGGGTTTTTCATGA CCAGAAACTCTCGTTTCCAAATCCAAAATAAAACCTGTTGATA CTGTTGCTAGCTTTCGCTTCAAACTCGAACTGTCGCAGTCTGAT TCACACAGATCAACAACTGGGTCGGCATGGCATCTCCACCTCC TCGCGGTCCGACCTGGGCTACTTCGGTAGGCTAAGGGAGAAGG GATCCAAA
DENV2 3neg gBlock	AAAAAGAATTCTAATACGACTCACTATAGACGCGGTTTCTCTC GCGTTTCAGCATATTGAAAGGCGTGTTTTTCGCCTTTTTCCGTT GGTTATTCATCAGAGATCTGCTCTCTAATTAAAAAACTGTTAGA ACTACGTTGAGCTTAGCTCCCTCAAAGAATCTGTCTTTGTCGGT CCACGTAGACTAACAACTGGGTCGGCATGGCATCTCCACCTCC TCGCGGTCCGACCTGGGCTACTTCGGTAGGCTAAGGGAGAAGG GATCCAAA

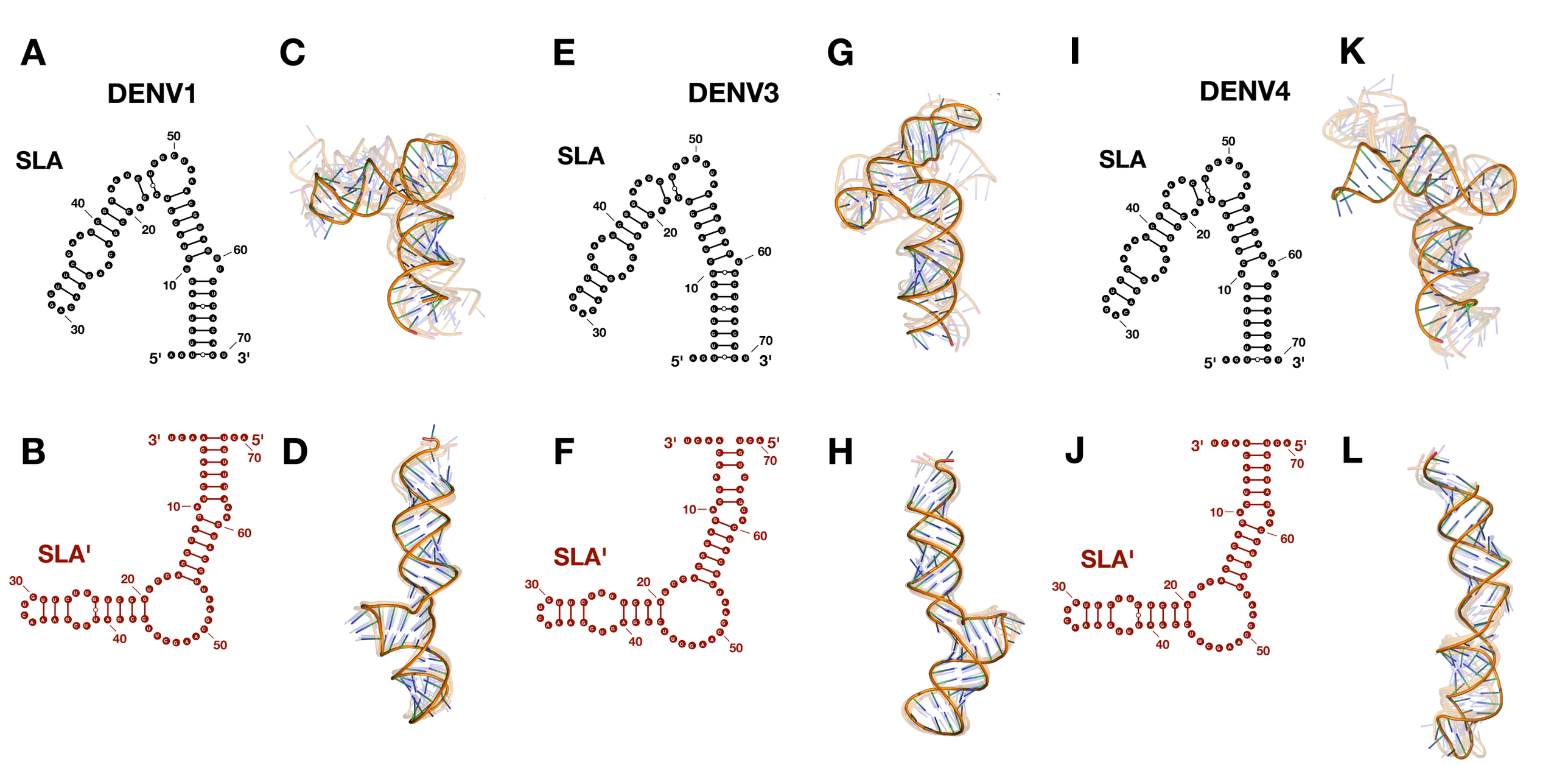

Figure S1. DENV1, DENV3, and DENV4 are predicted to form SLA′ at the 3′ termini of their negative strands. (A,E,I) Most stable predicted secondary structure for the first 70 nt at the 5′ terminus of the positive-strand for DENV1 (A), DENV3 (E) and DENV4 (I). (B,F,J) Most stable predicted secondary structure for the last 70 nt at the 3′ terminus of the negative-strand for DENV1 (B), DENV3 (F) and DENV4 (J). Tick marks represent 10 nt intervals. (C,G,K) RNA tertiary structure predictions for the first 70 nt at the 5′ terminus of the positive-strand for DENV1 (C), DENV3 (J) and DENV4 (K). (D,H,L) RNA tertiary structure predictions for the last 70 nt at the 3′ terminus of the negative-strand for DENV1 (D), DENV3 (H) and DENV4 (L). The highest confidence tertiary structure prediction is fully opaque, while the next four highest-ranked predictions are translucent.

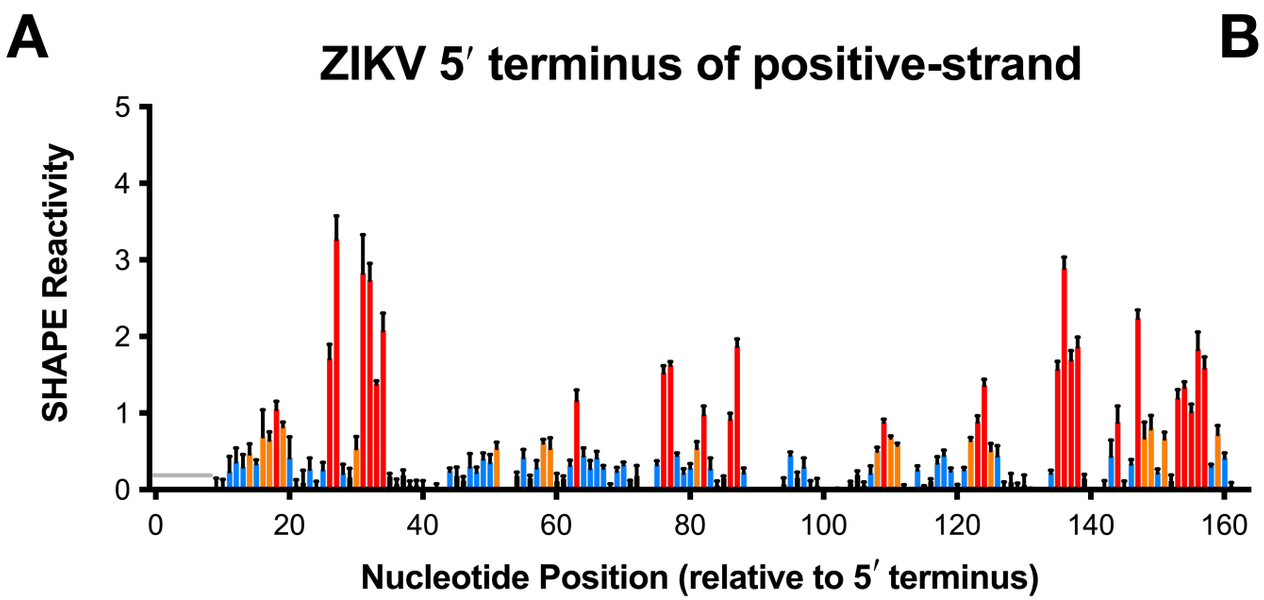

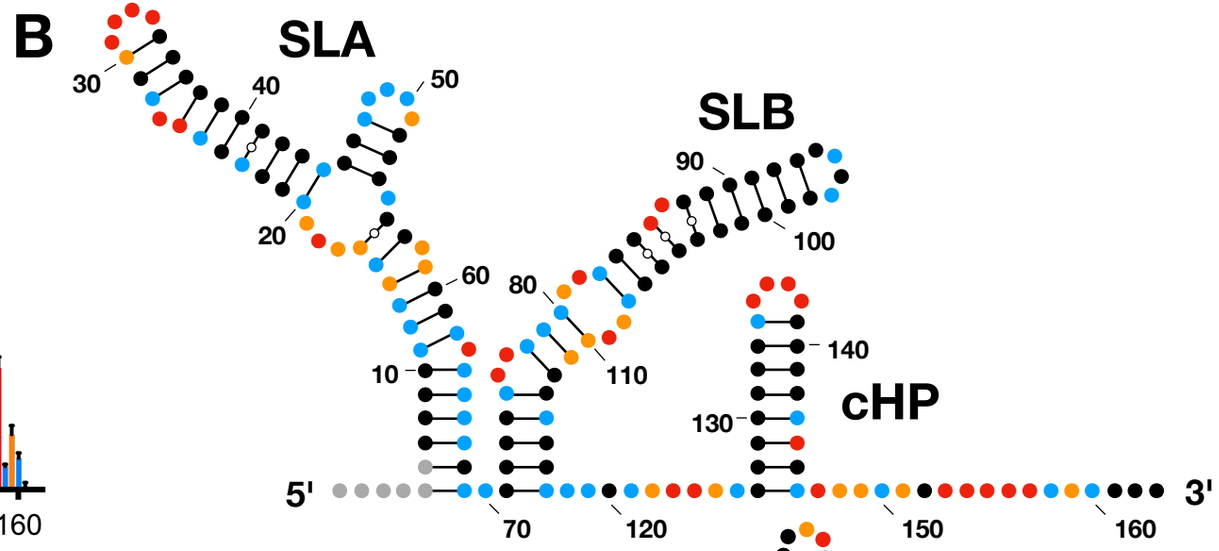

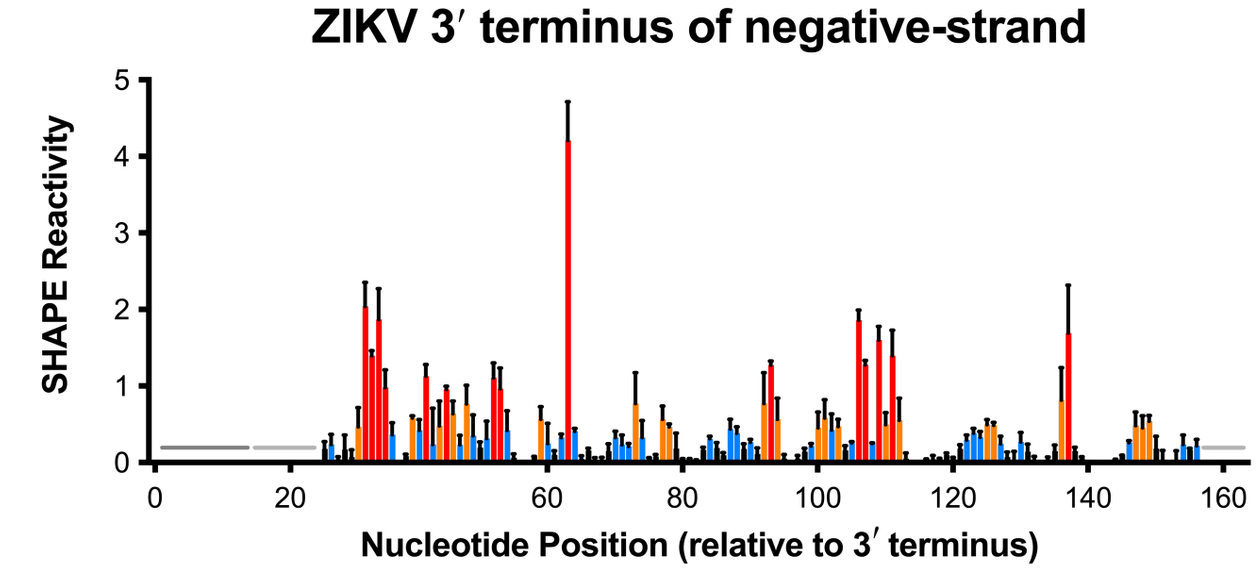

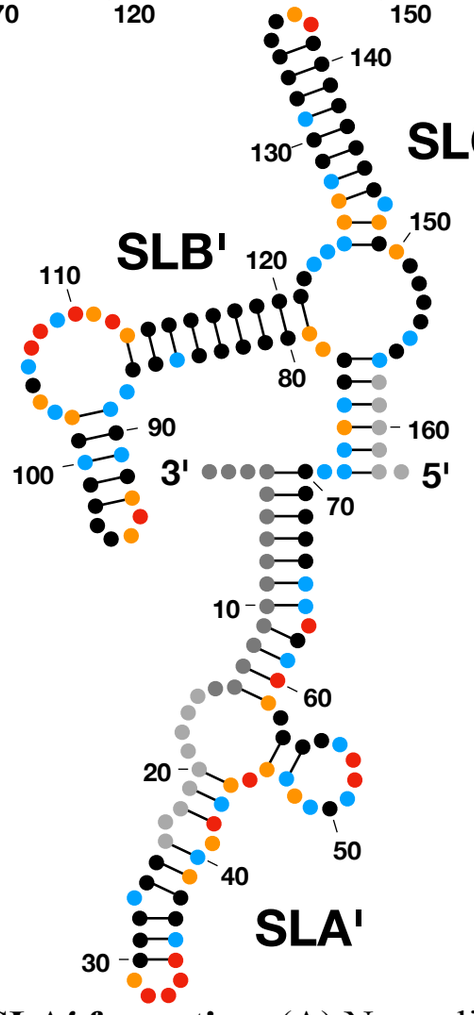

Figure S2. *In vitro* SHAPE analysis of the 3′ end of the negative-strand in ZIKV is consistent with SLA′ formation. (A) Normalized SHAPE reactivities of the first 163 nt at the 5′ terminus of the positive-strand of ZIKV. Data is shown as the normalized SHAPE reactivity from four biological replicates and error bars represent the standard error of the mean (SEM). Nucleotides with very low (≤ 0.2), low (0.2 - 0.4, blue), intermediate (0.4 - 0.85, orange), and high (≥ 0.85, red) SHAPE reactivity are indicated. Nucleotides 1-6 were omitted due to high background reactivity (light grey). (B) Prediction of the lowest free energy structure formed by the first 163 nt of the ZIKV positive-strand as constrained by the normalized SHAPE reactivity data from (A). Tick marks represent 10 nt intervals. (C) Normalized SHAPE reactivities of the last 163 nt at the 3′ terminus of the negative-strand of ZIKV. Data is shown as the normalized SHAPE reactivity from four biological replicates and error bars represent the SEM. Nucleotides 1-15 were bound by the primer (dark grey), and nucleotides 16-23 and 157-163 were omitted due to high background reactivity (light grey). (D) Prediction of the lowest free energy structure formed by the last 163 nt of the ZIKV negative-strand as constrained by the normalized SHAPE reactivity data from (C).

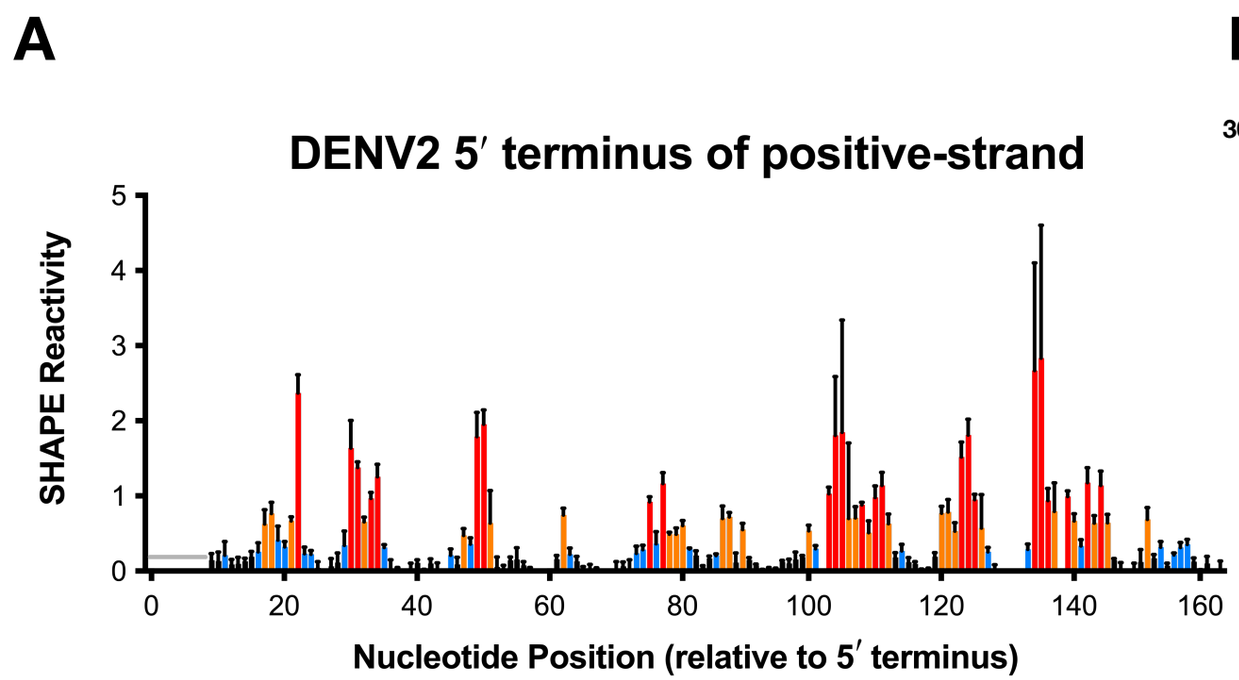

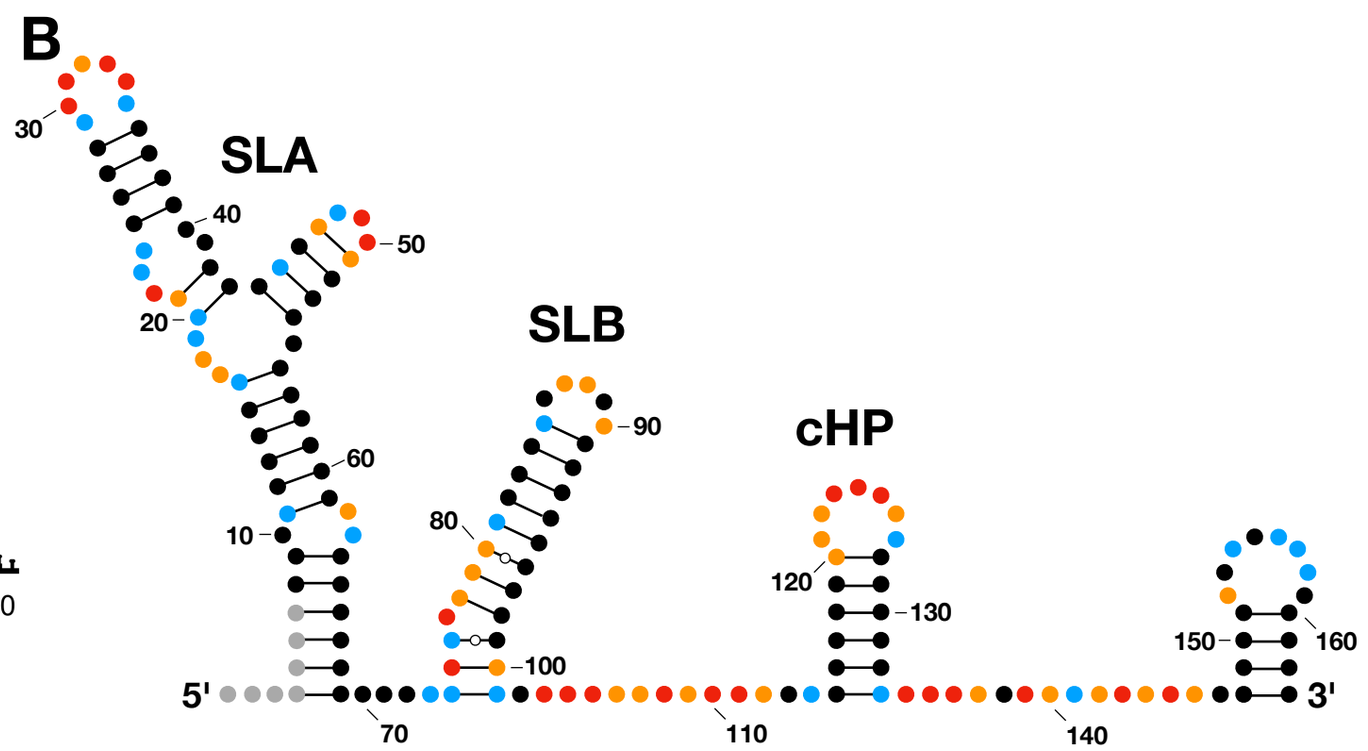

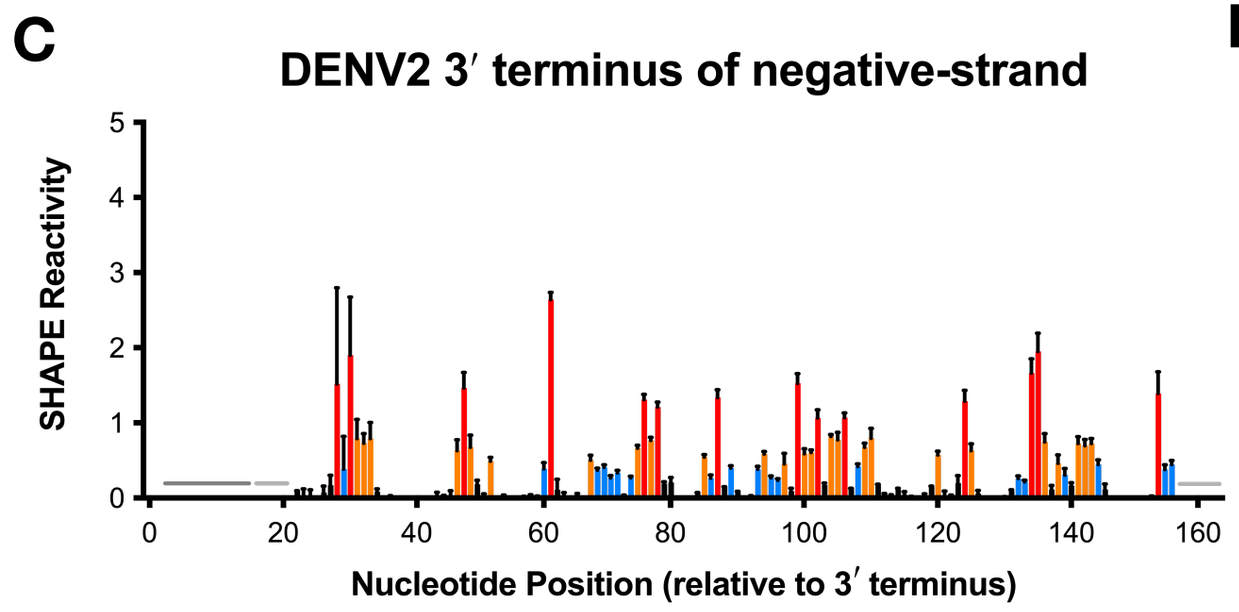

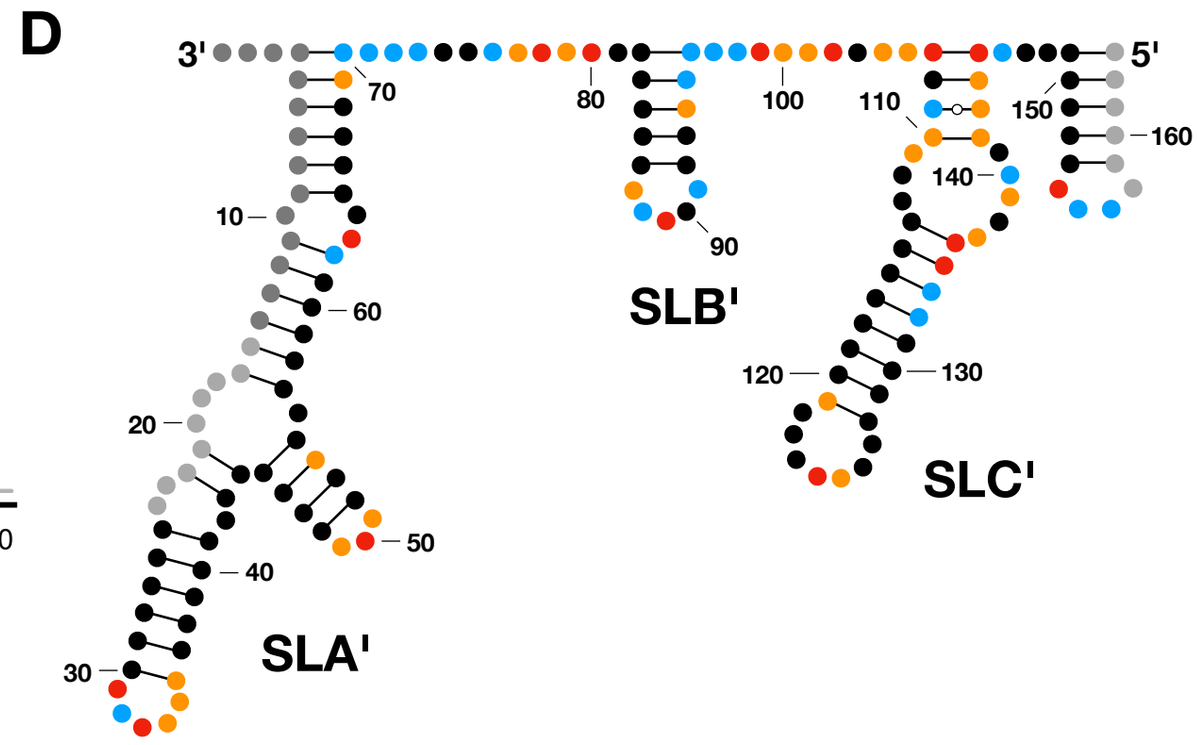

Figure S3. *In vitro* SHAPE analysis of the 3′ end of the negative strand in DENV2 is consistent with SLA′ formation. (A) Normalized SHAPE reactivities of the first 163 nt at the 5′ terminus of the positive-strand of DENV2. Data is shown as the normalized SHAPE reactivity from four biological replicates and error bars represent the SEM. Nucleotides with very low (≤ 0.2), low (0.2 - 0.4, blue), intermediate (0.4 - 0.85, orange), and high (≥ 0.85, red) SHAPE reactivity are indicated. Nucleotides 1-7 were omitted due to high background reactivity (light grey). (B) Prediction of the lowest free energy structure formed by the first 163 nt of the DENV2 positive-strand as constrained by the normalized SHAPE reactivity data from (A). Tick marks represent 10 nt intervals. (C) Normalized SHAPE reactivities of the last 163 nt at the 3′ terminus of the negative-strand of DENV2. Data is shown as the normalized SHAPE reactivity from four biological replicates and error bars represent the SEM. Nucleotides 1-15 were bound by the primer (dark grey), and nucleotides 16-24 and 157-163 were omitted due to high background reactivity (light grey). (D) Prediction of the lowest free energy structure formed by the last 70 nt of the DENV2 negative-strand as constrained by the normalized SHAPE reactivity data from (C).

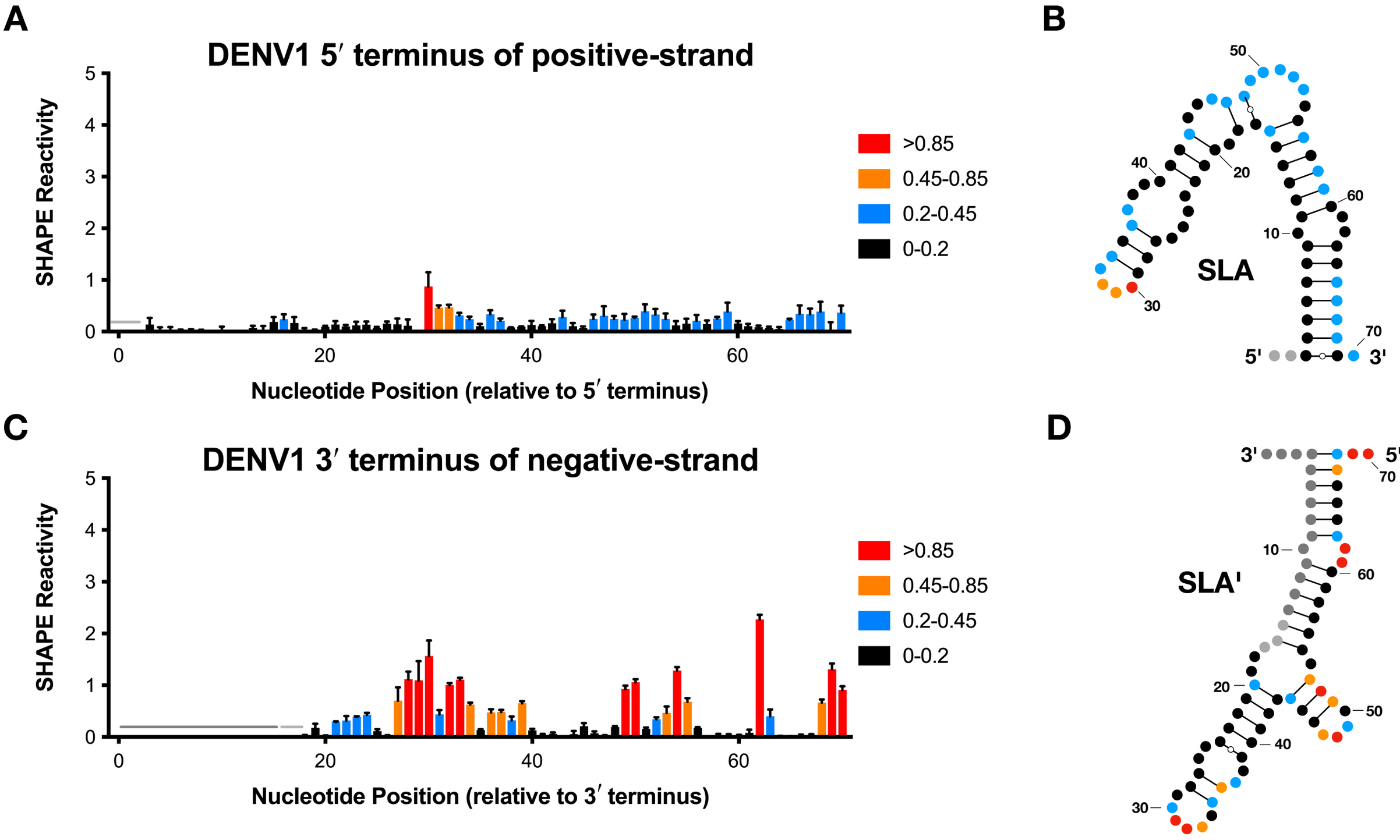

Figure S4. ***In vitro*** **SHAPE analysis of the 3′ terminus of the negative strand in DENV1 is consistent with SLA′ formation**. (A) Normalized SHAPE reactivities of the first 70 nt at the 5′ terminus of the positive-strand of DENV1. Data is shown as the normalized SHAPE reactivity from four biological replicates and error bars represent the SEM. Nucleotides with very low (≤ 0.2), low (0.2 - 0.4, blue), intermediate (0.4 - 0.85, orange), and high (≥ 0.85, red) SHAPE reactivity are indicated. Nucleotides 1-2 were omitted due to high background reactivity (light grey). (B) Prediction of the lowest free energy structure formed by the first 70 nt of the DENV1 positive-strand as constrained by the normalized SHAPE reactivity data from (A). Tick marks represent 10 nt intervals. (C) Normalized SHAPE reactivities of the last 70 nt at the 3′ terminus of the negative-strand of DENV1. Data is shown as the normalized SHAPE reactivity from four biological replicates and error bars represent the SEM. Nucleotides 1-15 were bound by the primer (dark grey), and nucleotides 16-18 were omitted due to high background reactivity (light grey). (D) Prediction of the lowest free energy structure formed by the last 70 nt of the DENV1 negative-strand as constrained by the normalized SHAPE reactivity data from (C).

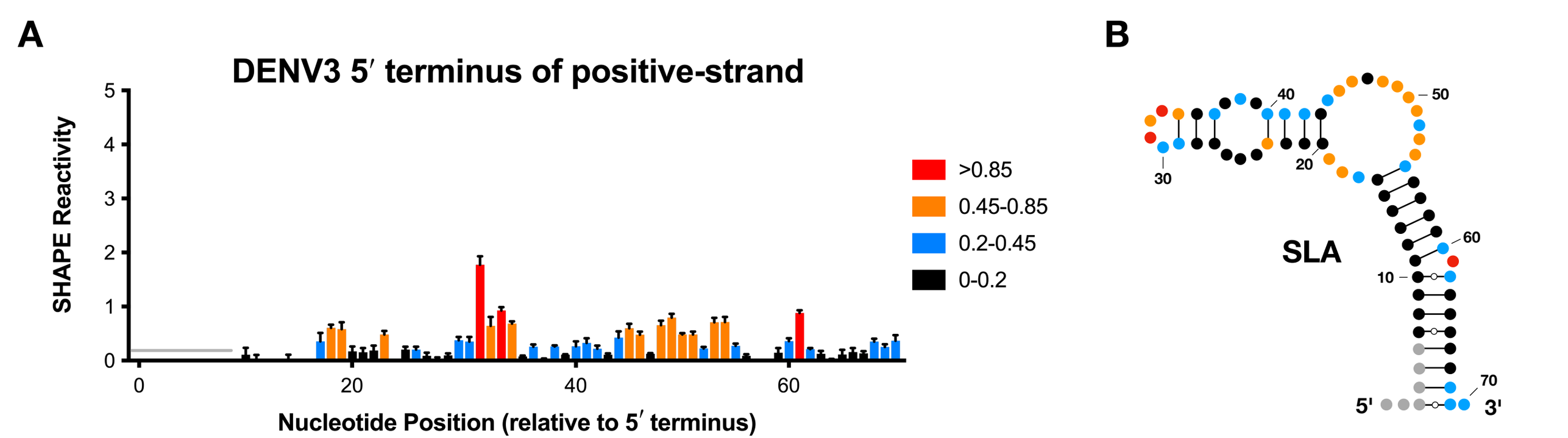

Figure S5. *In vitro* SHAPE analysis of the 3′ terminus of the negative strand in DENV3 is consistent with SLA′ formation. (A) Normalized SHAPE reactivities of the first 70 nt at the 5′ terminus of the positive-strand of DENV3. Data is shown as the normalized SHAPE reactivity from four biological replicates and error bars represent the SEM. Nucleotides with very low (≤ 0.2), low (0.2 - 0.4, blue), intermediate (0.4 - 0.85, orange), and high (≥ 0.85, red) SHAPE reactivity are indicated. Nucleotides 1-6 were omitted due to high background reactivity (light grey). (B) Prediction of the lowest free energy structure formed by the first 70 nt of the DENV3 positive-strand as constrained by the normalized SHAPE reactivity data from (A). Tick marks represent 10 nt intervals. (C) Normalized SHAPE reactivities of the last 70 nt at the 3′ terminus of the negative-strand of DENV3. Data is shown as the normalized SHAPE reactivity from four biological replicates and error bars represent the SEM. Nucleotides 1-15 were bound by the primer (dark grey), and nucleotides 16-20 were omitted due to high background reactivity (light grey). (D) Prediction of the lowest free energy structure formed by the last 70 nt of the DENV3 negative-strand as constrained by the normalized SHAPE reactivity data from (C).

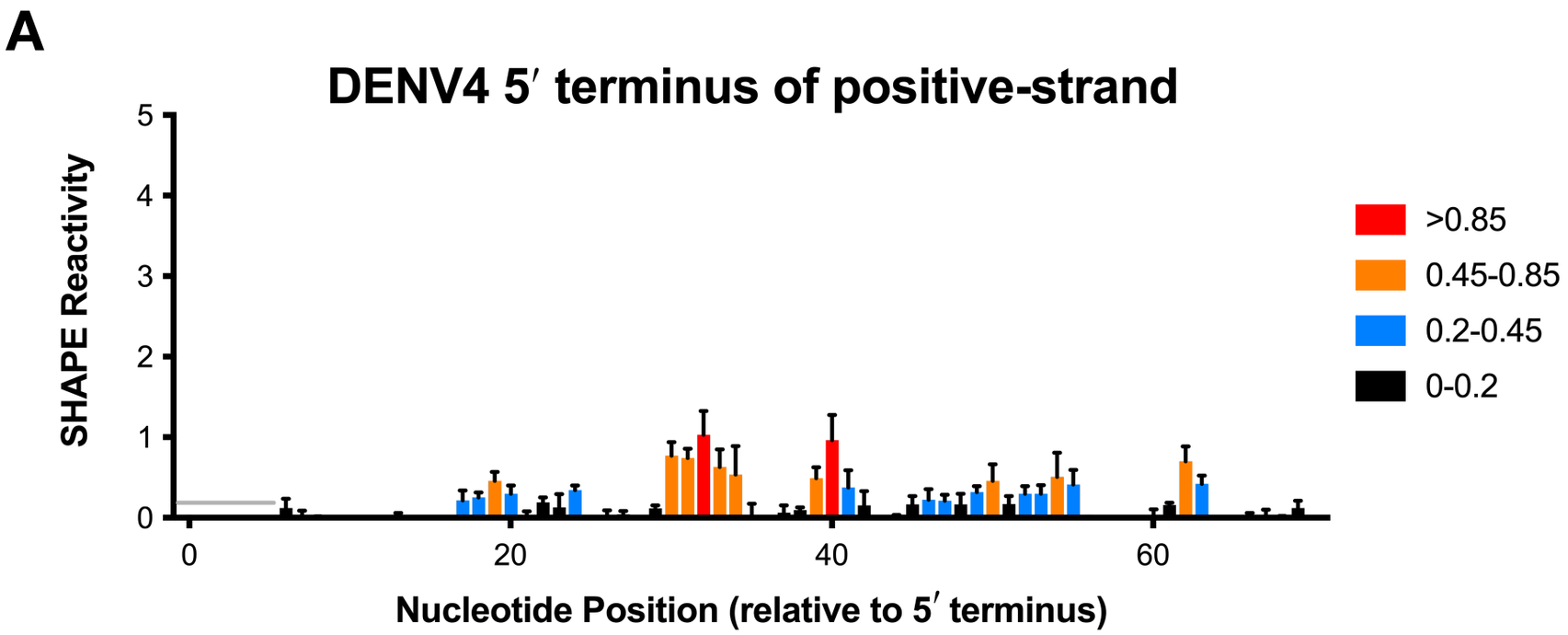

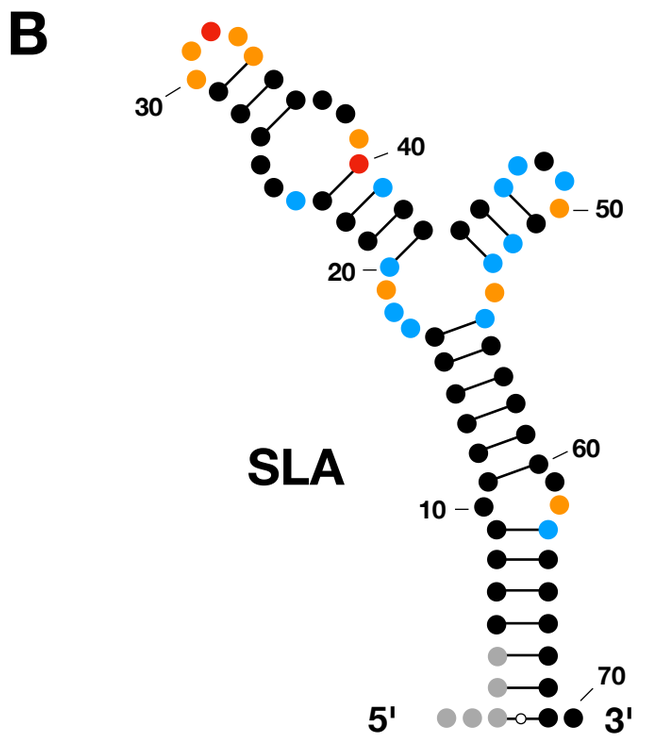

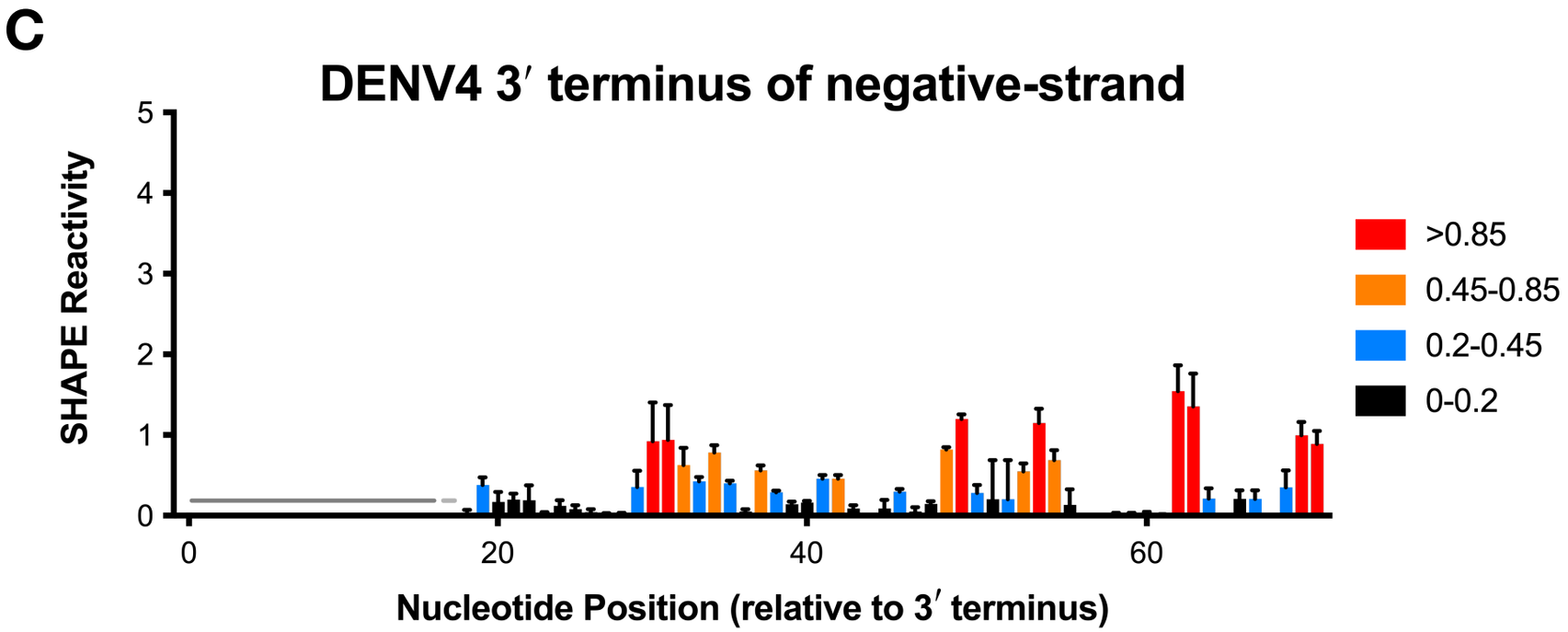

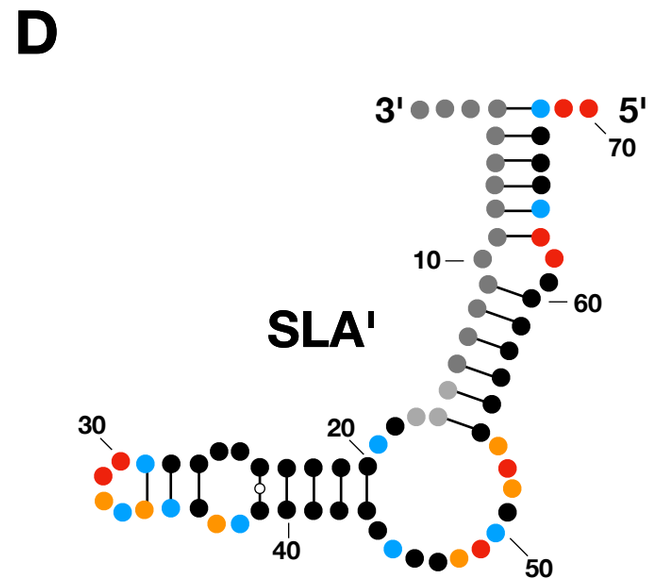

Figure S6. *In vitro* SHAPE analysis of the 3′ terminus of the negative strand in DENV4 is consistent with SLA′ formation. (A) Normalized SHAPE reactivities of the first 70 nt at the 5′ terminus of the positive-strand of DENV4. Data is shown as the normalized SHAPE reactivity from four biological replicates and error bars represent the SEM. Nucleotides with very low (≤ 0.2), low (0.2 - 0.4, blue), intermediate (0.4 - 0.85, orange), and high (≥ 0.85, red) SHAPE reactivity are indicated. Nucleotides 1-5 were omitted due to high background reactivity (light grey). (B) Prediction of the lowest free energy structure formed by the first 70 nt of the DENV4 positive-strand as constrained by the normalized SHAPE reactivity data from (A). Tick marks represent 10 nt intervals. (C) Normalized SHAPE reactivities of the last 70 nt at the 3′ terminus of the negative-strand of DENV4. Data is shown as the normalized SHAPE reactivity from four biological replicates and error bars represent the SEM. Nucleotides 1-15 were bound by the primer (dark grey), and nucleotides 16-18 were omitted due to high background reactivity (light grey). (D) Prediction of the lowest free energy structure formed by the last 70 nt of the DENV4 negative-strand as constrained by the normalized SHAPE reactivity data from (C).

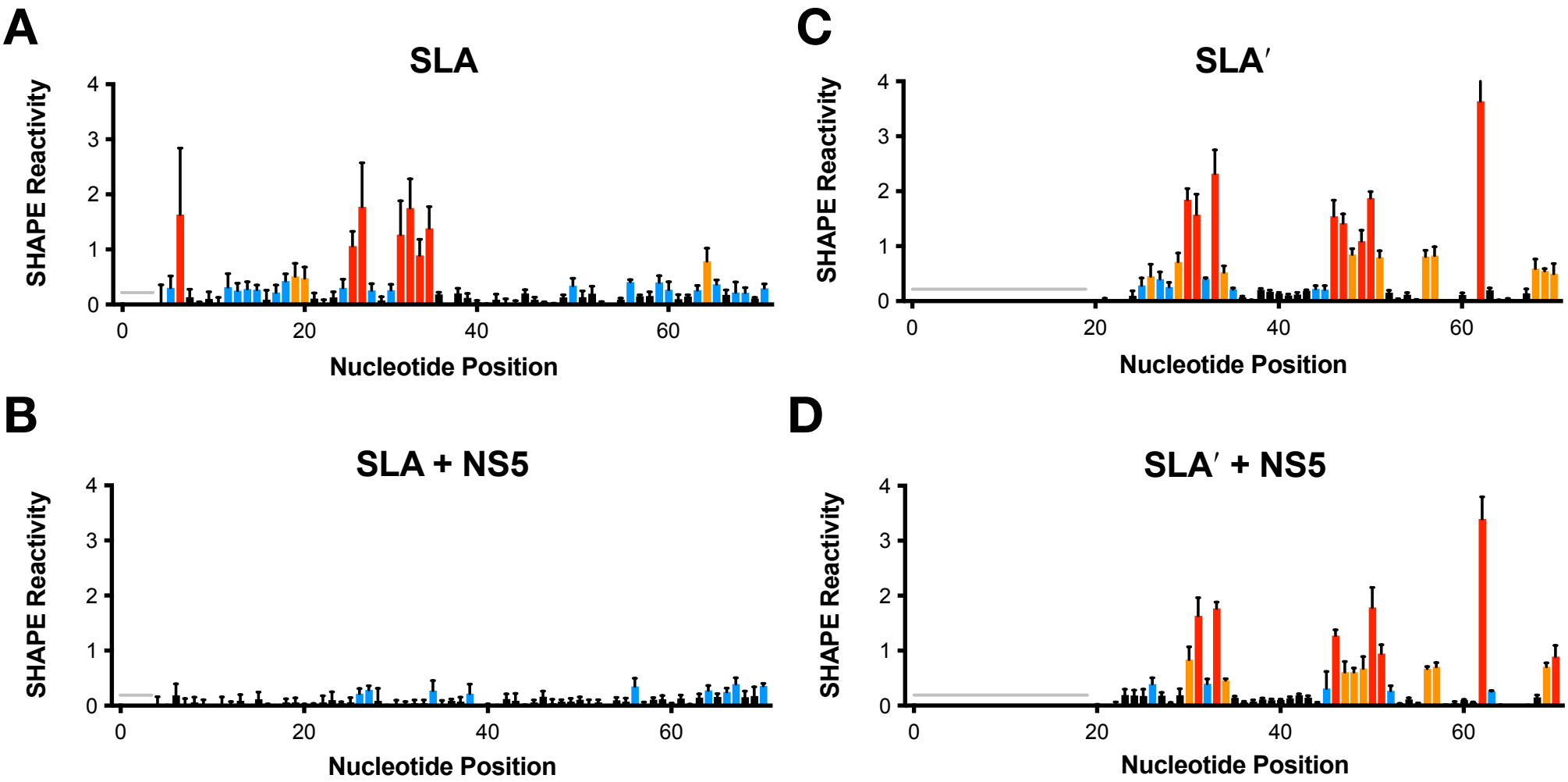

Figure S7. *In vitro* SHAPE analysis of ZIKV SLA and SLA′ in the presence and absence of NS5. (A-B) Normalized SHAPE reactivities of the first 70 nt at the 5′ terminus of the positive-strand of ZIKV in the absence or presence of NS5. Data is shown as the normalized SHAPE reactivity from four biological replicates and error bars represent the SEM. Nucleotides with very low (≤ 0.2), low (0.2 - 0.4, blue), intermediate (0.4 - 0.85, orange), and high (≥ 0.85, red) SHAPE reactivity are indicated. Nucleotides 1-6 were omitted due to high background reactivity (light grey). (C-D) Normalized SHAPE reactivities of the last 70 nt at the 3′ terminus of the positive-strand of ZIKV in the absence or presence of NS5. Data is shown as the normalized SHAPE reactivity from four biological replicates and error bars represent the SEM. Nucleotides are coloured as in (A-B). Nucleotides 1-15 were bound by the primer, and nucleotides 16-20 were omitted due to high background reactivity.

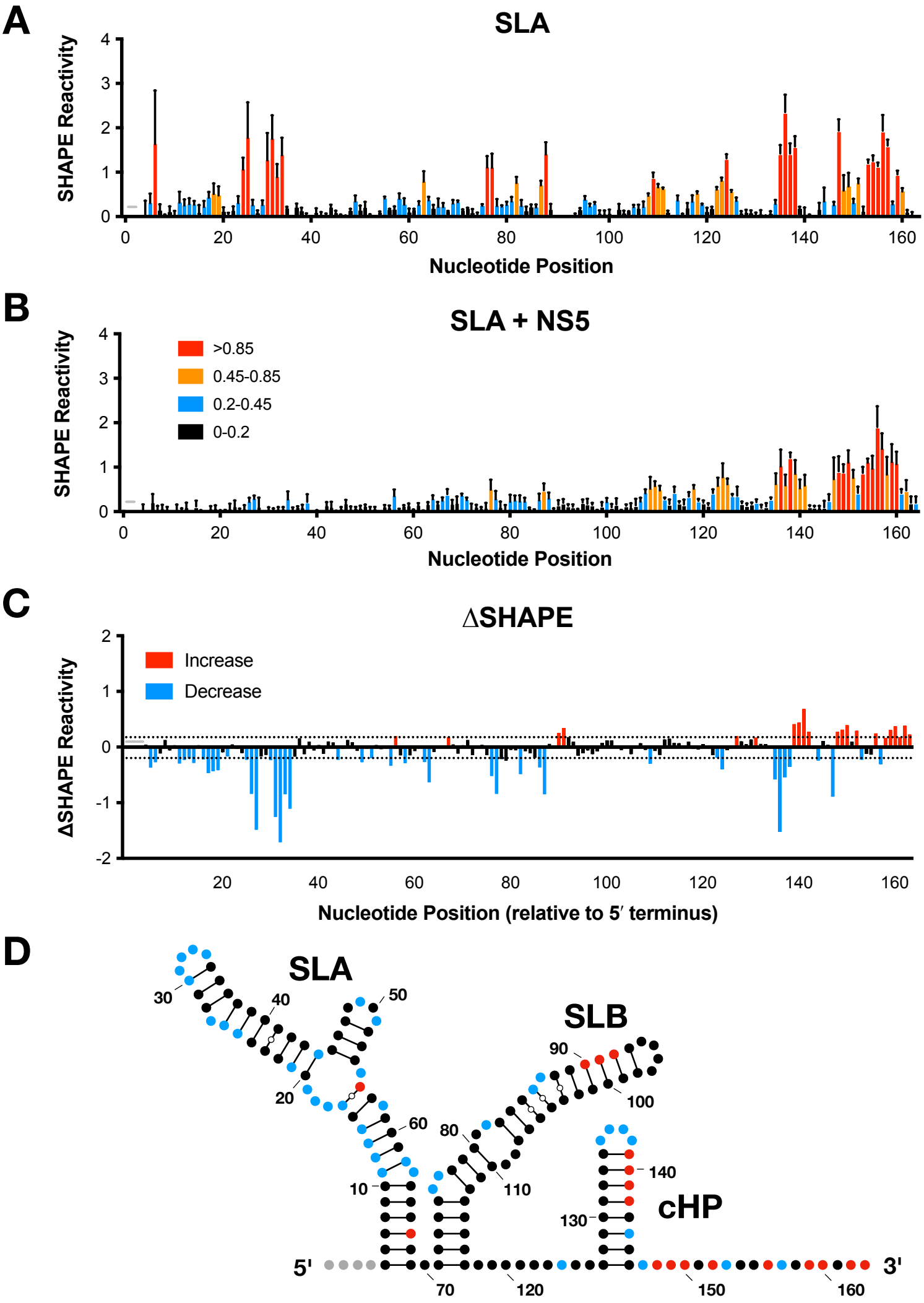

Figure S8. *In vitro* ΔSHAPE analysis of the ZIKV 5′ terminus of the positive-strand in the presence and absence of NS5. (A-B) Normalized SHAPE reactivities of the first 163 nt at the 5′ terminus of the positive-strand of ZIKV in the (A) absence or (B) presence of NS5. Data is shown as the normalized SHAPE reactivity from four biological replicates and error bars represent the SEM. Nucleotides with very low (≤ 0.2), low (0.2 - 0.4, blue), intermediate (0.4 - 0.85, orange), and high (≥ 0.85, red) SHAPE reactivity are indicated. Nucleotides 1-3 were omitted due to high background reactivity (light grey). (C) ΔSHAPE reactivity plots for the first 163 nt of the 5′ terminus of the positive-strand and in the presence or absence of ZIKV NS5 (i.e. ΔSHAPE = NS5:RNA reactivity – RNA only reactivity). Data is shown as the normalized change in SHAPE reactivity upon NS5 binding at each nucleotide position from four biological replicates. Significant (> magnitude of the average ΔSHAPE reactivity) increases (red) and decreases (blue) in SHAPE reactivity upon NS5 binding are indicated. The baseline significance is indicated with a dashed line. (D) ΔSHAPE reactivity data from (C) mapped onto the predicted structure of the first 163 nt at the 5′ terminus of the positive-strand of ZIKV. Tick marks represent 10 nt intervals.

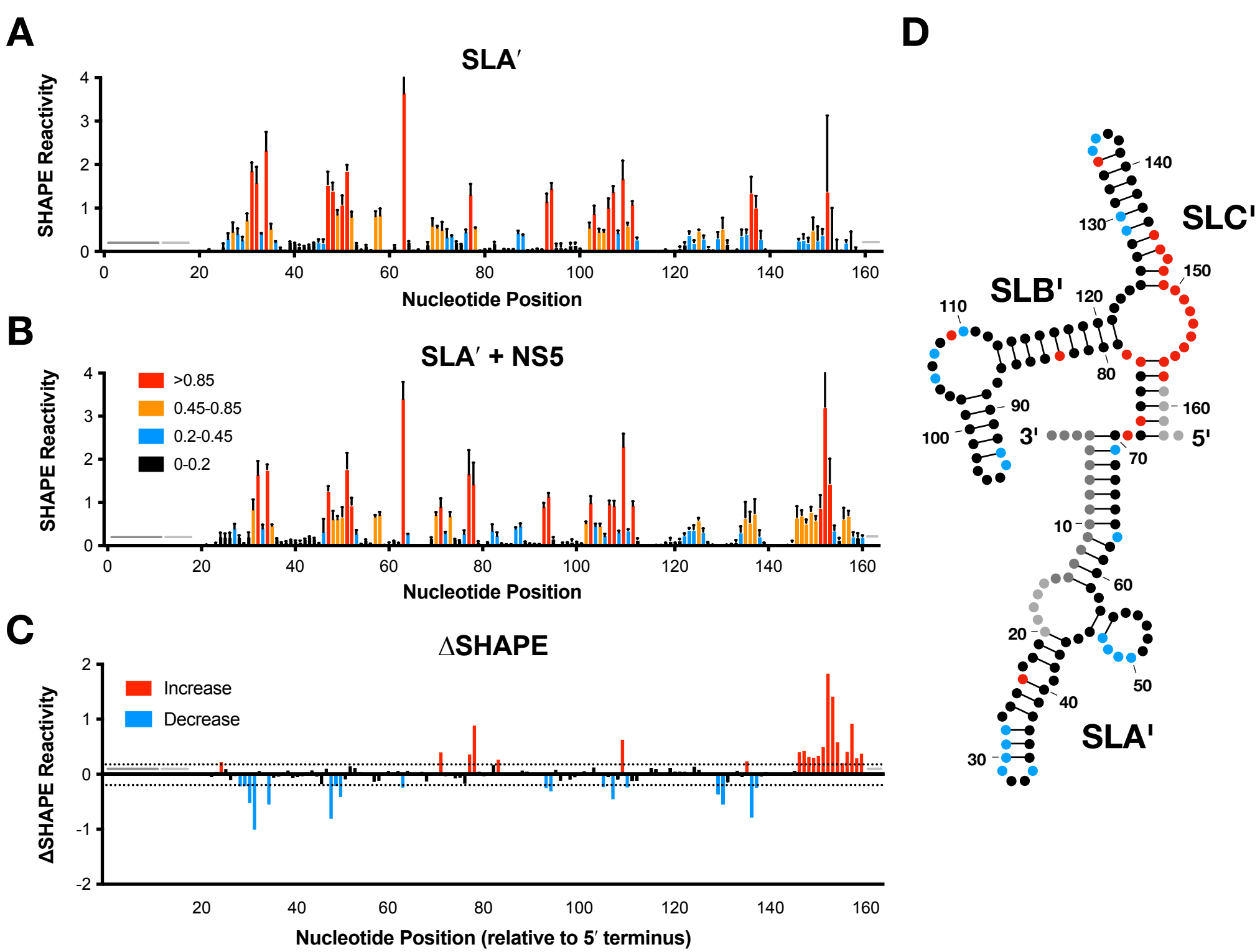

Figure S9. *In vitro* ΔSHAPE analysis of the ZIKV 3′ terminus of the negative-strand in the presence and absence of NS5. (A-B) Normalized SHAPE reactivities of the last 163 nt at the 3′ terminus of the negative-strand of ZIKV in the (A) absence or (B) presence of NS5. Data is shown as the normalized SHAPE reactivity from four biological replicates and error bars represent the SEM. Nucleotides with very low (≤ 0.2), low (0.2 - 0.4, blue), intermediate (0.4 - 0.85, orange), and high (≥ 0.85, red) SHAPE reactivity are indicated. Nucleotides 1-15 were bound by the primer (dark grey), and nucleotides 16-21 were omitted due to high background reactivity (light grey). (C) ΔSHAPE reactivity plots for the last 163 nt of the 3′ terminus of the negative-strand in the presence or absence of ZIKV NS5 (i.e. ΔSHAPE = NS5:RNA reactivity – RNA only reactivity). Data is shown as the normalized change in SHAPE reactivity upon NS5 binding at each nucleotide position from four biological replicates. Significant (> magnitude of the average ΔSHAPE reactivity) increases (red) and decreases (blue) in SHAPE reactivity upon NS5 binding are indicated. The baseline significance is indicated with a dashed line. (D) ΔSHAPE reactivity data from (C) mapped onto the predicted structure of the last 163 nt at the 3′ terminus of the negative-strand of ZIKV. Tick marks represent 10 nt intervals.

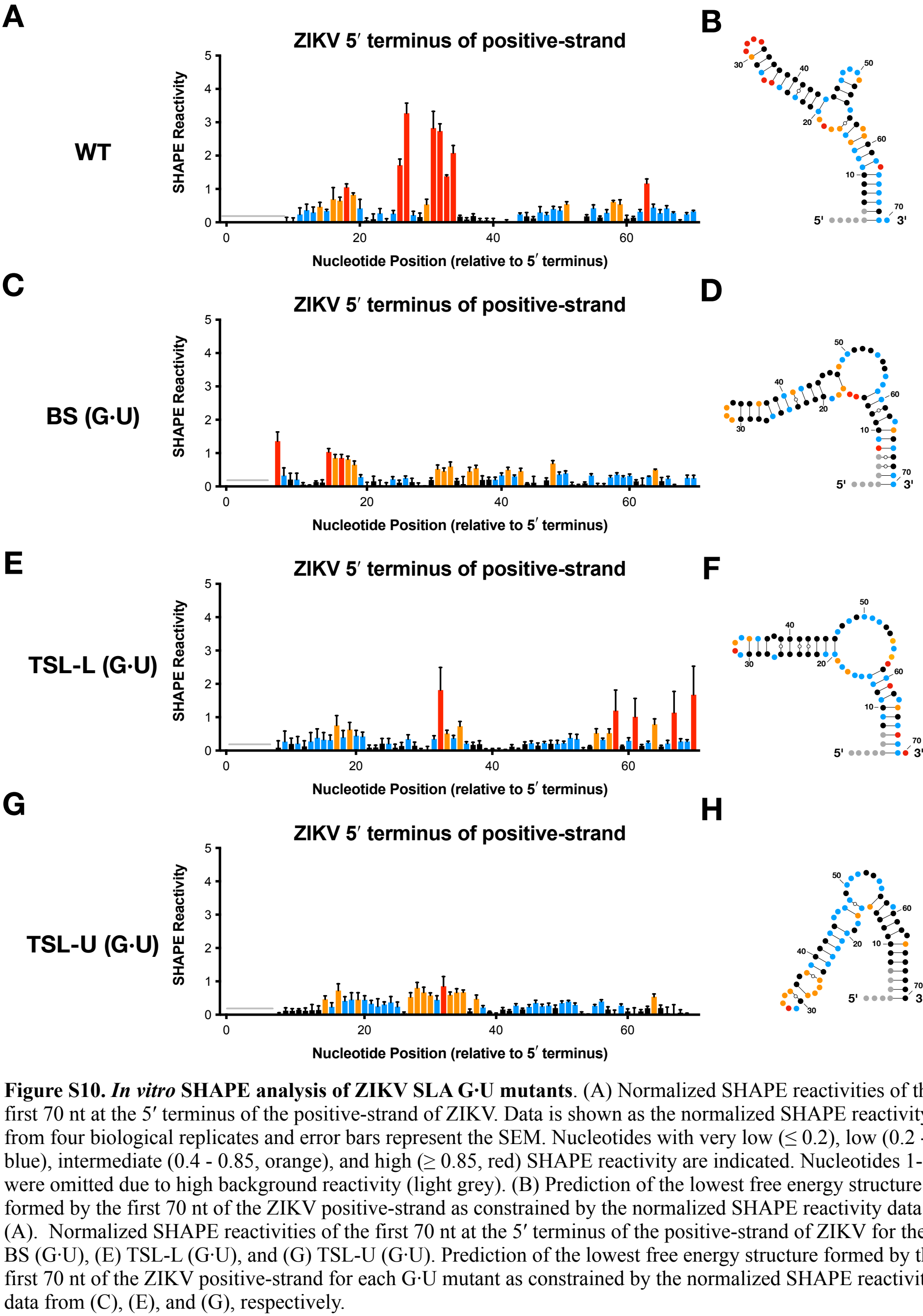

Figure S10. *In vitro* SHAPE analysis of ZIKV SLA G·U mutants. (A) Normalized SHAPE reactivities of the first 70 nt at the 5′ terminus of the positive-strand of ZIKV. Data is shown as the normalized SHAPE reactivity from four biological replicates and error bars represent the SEM. Nucleotides with very low (≤ 0.2), low (0.2 - 0.4, blue), intermediate (0.4 - 0.85, orange), and high (≥ 0.85, red) SHAPE reactivity are indicated. Nucleotides 1-7 were omitted due to high background reactivity (light grey). (B) Prediction of the lowest free energy structure formed by the first 70 nt of the ZIKV positive-strand as constrained by the normalized SHAPE reactivity data from (A). Normalized SHAPE reactivities of the first 70 nt at the 5′ terminus of the positive-strand of ZIKV for the (C) BS (G·U), (E) TSL-L (G·U), and (G) TSL-U (G·U). Prediction of the lowest free energy structure formed by the first 70 nt of the ZIKV positive-strand for each G·U mutant as constrained by the normalized SHAPE reactivity data from (C), (E), and (G), respectively.

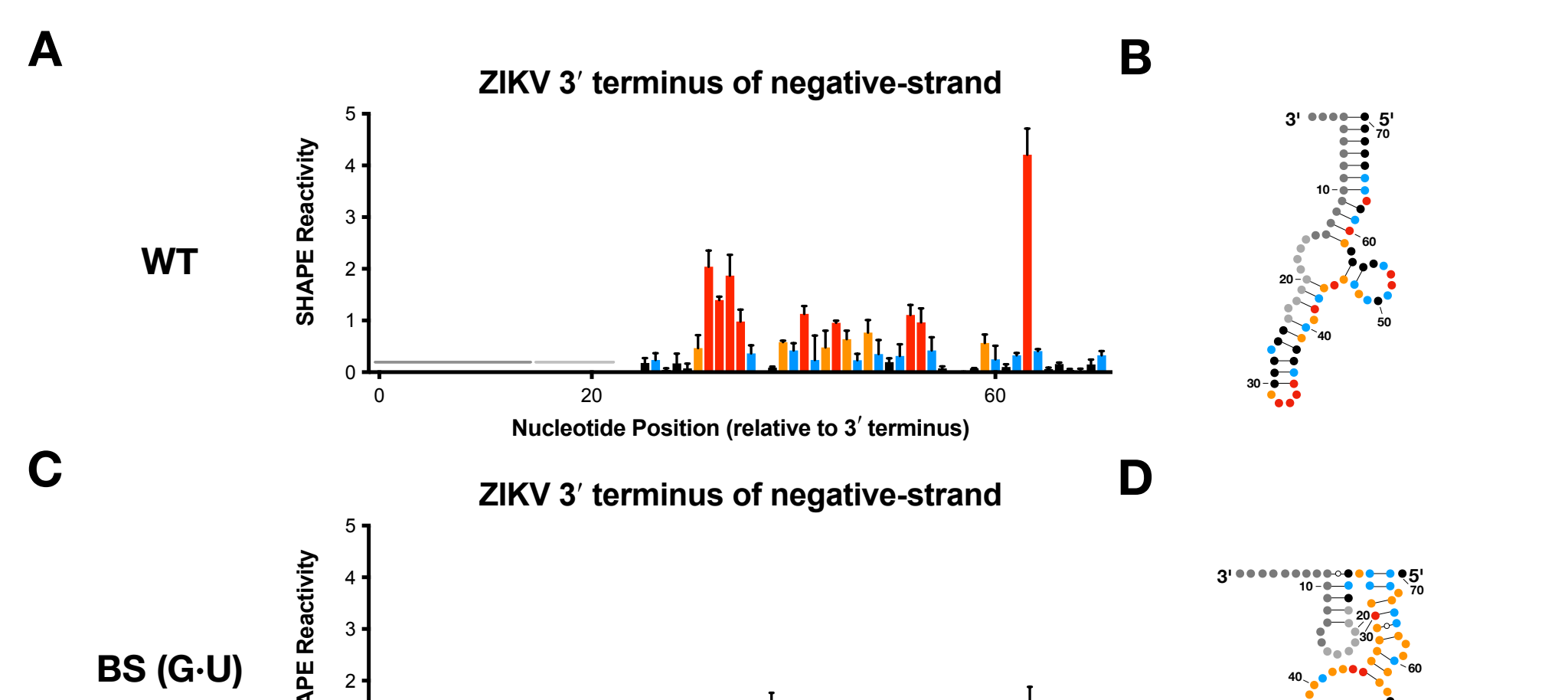

Figure S11. *In vitro* SHAPE analysis of ZIKV SLA′ G·U mutants. (A) Normalized SHAPE reactivities of the last 70 nt at the 3′ terminus of the negative-strand of ZIKV. Data is shown as the normalized SHAPE reactivity from four biological replicates and error bars represent the SEM. Nucleotides with very low (≤ 0.2), low (0.2 - 0.4, blue), intermediate (0.4 - 0.85, orange), and high (≥ 0.85, red) SHAPE reactivity are indicated. Nucleotides 1-15 were bound by the primer (dark grey), and nucleotides 16-21 were omitted due to high background reactivity (light grey). (B) Prediction of the lowest free energy structure formed by the last 70 nt of the ZIKV negative-strand as constrained by the normalized SHAPE reactivity data from (A). Normalized SHAPE reactivities of the last 70 nt at the 3′ terminus of the negative-strand of ZIKV for the (C) BS (G·U), (E) TSL-L (G·U), and (G) TSL-U (G·U). Prediction of the lowest free energy structure formed by the last 70 nt of the ZIKV negative-strand for each G·U mutant as constrained by the normalized SHAPE reactivity data from (C), (E), and (G), respectively.